

**20th International Conference on
Harmonisation within Atmospheric Dispersion Modelling for Regulatory Purposes
14-18 June 2020, Tartu, Estonia**

**ROBUSTNESS OF A RECONSTRUCTED SOURCE TERM TO METEOROLOGICAL DATA
AND DEPOSITION SCHEME: APPLICATION TO THE CASE STUDY OF RUTHENIUM-106
RELEASE IN FALL 2017.**

Olivier Saunier¹, Denis Quélo¹, Arnaud Quérel¹ and Jérôme Groell¹

¹IRSN, Fontenay-aux-Roses, France

Abstract: In the fall 2017, a rare episode of low levels of ruthenium was observed in the atmosphere of most European countries. IRSN used variational inverse modelling techniques to identify the origin and to assess the duration and the magnitude of the releases. The source reconstruction was performed using three-hourly operational meteorological data from Météo-France with 0.5° spatial resolution. The approach made it possible to identify the most likely geographical origin of the release with a reasonable level of confidence. However, the dispersion of the simulated plume highlighted that air concentration measurements were underestimated in Italy whereas deposition measurements were strongly underestimated in Scandinavia and overestimated in Hungary. In this paper, variational inverse methods are implemented combining new sources of meteorological data and new deposition schemes. In addition, Gaussian and log-normal errors are considered to solve the inverse problem and the impacts on the source reconstruction are investigated. The results confirm that the most likely release location is situated in the southern Urals. The period and duration of the release are still uncertain. Furthermore, source term reconstructed using ECMWF meteorological fields and log-normal errors help to significantly improve the agreement between observed and modelled air concentrations.

Key words: Ruthenium-106, source reconstruction, inverse modelling.

INTRODUCTION

In the past few years, several unusual detections events of radionuclides in the atmosphere have been reported in Europe while the geographical origin was unknown. These situations usually involved small amounts of radionuclides released in the environment and the concentrations levels measured were too low to have any impact on human health and environment. For such situations, the Institute for Radiological Protection and Nuclear Safety (IRSN) uses atmospheric transport models to analyse the event in more detail. The aim is, in particular, to pinpoint the origin, to assess the duration and the magnitude of the release. In fall 2017, abnormal Ruthenium-106 (¹⁰⁶Ru) detections were reported by the majority of European countries, the origin of the release being unknown. Inverse modelling methods which combine field measurements with atmospheric transport modelling have proven to be appropriate for the ¹⁰⁶Ru source identification (Saunier et al. 2019, Dumont le Brazidec et al. 2020, Western et al. 2020, Tichy et al. 2020). On the currently available inverse modelling approaches at IRSN, variational deterministic methods are suitable in operational use since they are able to quickly provide an optimal solution. In this study, the deterministic inverse methods implemented in Saunier et al. (2019) are applied using combination of two sources of meteorological fields and four deposition schemes. The minimization of the cost function associated with the inverse problem is performed assuming two different choices on errors. The objective is to identify the most influential parameters affecting the reconstructed source by inverse modelling and to determine, if possible, a relevant configuration that improves the realism of the simulations.

OBSERVATIONS

Ruthenium-106 was observed between the end of September and mid-October 2017 in the atmosphere of 31 countries on the European continent at levels ranging from a few $\mu\text{Bq}/\text{m}^3$ to more than 170 mBq/m^3 (Masson et al. 2019). Only stations located in Western Europe (Portugal, Spain, Great Britain, Benelux and Northern Ireland) did not report detections of ¹⁰⁶Ru above detection limits. In this study, more than 1000 air concentration measurements are used within the inverse procedure to pinpoint the origin of the release and to evaluate the total quantities of ¹⁰⁶Ru emitted to the atmosphere. In addition to the air concentration

measurements, deposition was also measured in a number of European countries. A number of daily deposition observations were recorded in the Russian Federation. In Europe, the highest cumulated deposits were recorded in Scandinavia with levels of up to 90 Bq/m² in Finland. Deposition of ¹⁰⁶Ru was also reported from Poland, Hungary, Austria, Italy and the Czech Republic, with a few Bq/m² of ¹⁰⁶Ru. All these deposition measurements are not taken into account in the inverse procedure but are used *a posteriori* to validate the simulations.

SOURCE RECONSTRUCTION METHODOLOGY

The approach used is described in details in Saunier et al. (2019). It is first assumed that the release occurred somewhere between Western Europe and Russian Federation. For computation time reasons, the domain likely to contain the source is divided into a set of 336 cells. Each centre of cell mesh is then considered to be a potential source of release. Dimensions of the domain including the potential sources are [26E, 66E], [35N, 65N] with 2° × 2° resolution. For each potential source, a source term is assessed by inverse modelling using a variational approach assuming that the measurement vector can be described as a linear model with a source-receptor matrix and unknown source term vector σ :

$$\mu = \mathbf{H}\sigma + \epsilon \quad (1)$$

The \mathbf{H} source-receptor matrix is the Jacobian matrix of the transport model and the vector ϵ represents a combined model-representation-instrumental error. Errors ϵ may be assumed to be Gaussian, following a normal distribution. Assuming Gaussian errors, the source term can be assessed by minimizing the cost function $J_G(\sigma)$ which measures the differences between the model predictions $\mathbf{H}\sigma$ and the real measurements μ :

$$J_G(\sigma) = \frac{1}{2}(\mu - \mathbf{H}\sigma)^T \mathbf{R}^{-1}(\mu - \mathbf{H}\sigma) \quad (2)$$

where $\mathbf{R} = E[\epsilon\epsilon^T]$ is the error covariance matrix associated with the error. It is well known that the source-receptor relationship (1) constitutes an ill-posed inverse problem and its resolution may fail particularly where the number of observations is limited. That is why a background term is usually added in the cost function (2). However, as described in Saunier et al. (2019), the number of available ¹⁰⁶Ru air concentration measurements is sufficiently high avoiding the need of an additional background term. One disadvantage of Gaussian errors is to give more weight to the high concentration values than to the low values. One possibility for overcoming this difficulty is to choose a log-normal distribution of errors resulting in the cost function $J_{LN}(\sigma)$:

$$J_{LN}(\sigma) = \frac{1}{2}(\ln(\mu) - \ln(\mathbf{H}\sigma))^T \mathbf{R}^{-1}(\ln(\mu) - \ln(\mathbf{H}\sigma))$$

In order to mitigate the influence of small concentration values, a threshold θ ($\theta = 1$ mBq/m³) is introduced in the cost function:

$$J_{LN}(\sigma) = \frac{1}{2}(\ln(\mu + \theta) - \ln(\mathbf{H}\sigma + \theta))^T \mathbf{R}^{-1}(\ln(\mu + \theta) - \ln(\mathbf{H}\sigma + \theta))$$

In this study, we have chosen to consider both log-normal and Gaussian errors, it is assumed that \mathbf{R} is diagonal and the error variance is the same for all diagonal elements of the matrix. The minimization of $J_G(\sigma)$ and $J_{LN}(\sigma)$ is equivalent to minimizing:

$$J_G(\sigma) = \frac{1}{2}(\mu - \mathbf{H}\sigma)^T(\mu - \mathbf{H}\sigma)$$

$$J_{LN}(\sigma) = \frac{1}{2}(\ln(\mu + \theta) - \ln(\mathbf{H}\sigma + \theta))^T(\ln(\mu + \theta) - \ln(\mathbf{H}\sigma + \theta))$$

The both cost functions are directly minimized using the L-BFGS-B limited-memory quasi-Newton minimizer by enforcing the positivity of the source. Then, for each inverted source, the agreement between modelled and observed air concentration measurements is then assessed using the factor 2 indicator (FAC2). FAC2 is the proportion of the simulated activity concentrations calculated using the reconstructed source that are within a factor of 2 of the observed values.

MODEL SET-UP

The Eulerian model IdX is used to simulate the radionuclide dispersion and to therefore construct the set of source-receptor matrixes \mathbf{H} on the whole domain containing the potential sources. The IdX model is part of

IRSN's C3X operational platform (Tombette et al. 2014). It has been applied to deal with massive accidental releases into the environment (Quélo et al., 2007, Saunier et al., 2013) and minor radionuclide detection events (Masson et al. 2018). IdX takes into account dry and wet deposition as well as radioactive decay and fission. Two sources of meteorological fields are considered:

- Hourly meteorological data from ECMWF (European Centre for Medium-Range Weather Forecasts) with 0.28125° resolution,
- Three-hourly meteorological data from Météo-France with 0.5° resolution.

Dry deposition is modelled by simple scheme with a constant deposition velocity whereas the wet scavenging is parameterized in the form $\Lambda = \Lambda_s I$ where I is the rain intensity (mm h^{-1}). In this study, 4 deposition schemes are used, the parametrizations are described in Table 1. In order to quantify the impact of the meteorological fields, the deposition scheme and the choice of the cost function on the source reconstruction, 8 source-receptor matrixes H_k which represent all combinations of meteorological data and deposition schemes are built at each centre of cell. In total, 336×8 source-receptor matrixes H_k are built assuming that the source reconstruction period is between September 22 and October 13 with daily time intervals. This leads to perform $336 \times 8 \times 21 = 56448$ forward simulations with IdX.

Table 1: Deposition schemes used for source reconstruction. Λ is the scavenging coefficient (s^{-1})

	dep_ref (Saunier et al. 2019)	dep1 (Quelo et al. 2021)	dep2	dep3
Dry deposition	$v_{\text{dep}} = 2.10^{-3} \text{ m.s}^{-1}$	$v_{\text{dep}} = 2.10^{-3} \text{ m.s}^{-1}$	$v_{\text{dep}} = 1.10^{-3} \text{ m.s}^{-1}$	$v_{\text{dep}} = 1.10^{-3} \text{ m.s}^{-1}$
Wet deposition – below-cloud (washout)	$\Lambda = 5 \times 10^{-5} I$			
Wet deposition – in-cloud (rainout)	$\Lambda = 5 \times 10^{-5} I$	$\Lambda = 5 \times 10^{-4} I^{0.64}$	$\Lambda = 5 \times 10^{-5} I$	$\Lambda = 5 \times 10^{-4} I^{0.64}$

RESULTS

Source location

Figure 1 shows that, when ECMWF meteorological fields are used, the highest FAC2 values are obtained in the Russian Federation, in the southern Urals region. Indeed, the FAC2 values exceed 40% in this geographical area, which indicates a good agreement between simulated and observed concentrations.

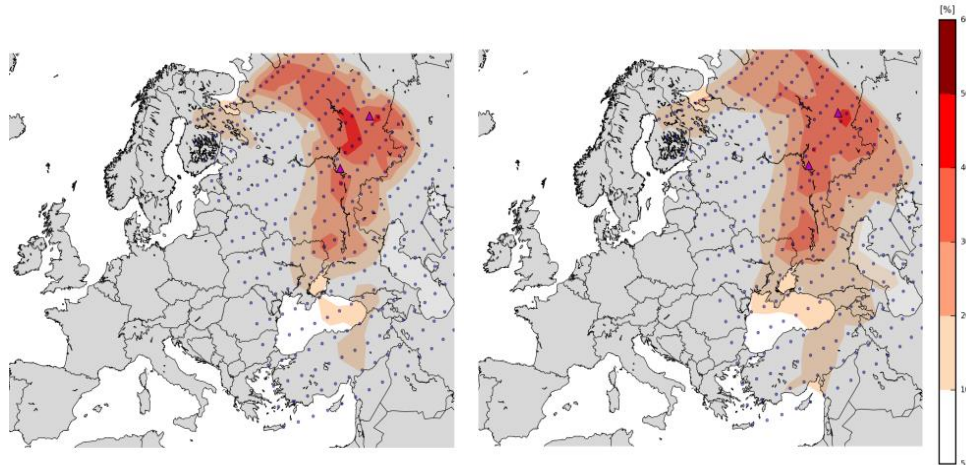


Figure 1: Percentage of simulated air concentrations that are within a factor of 2 of observed values. ECMWF meteorological fields and dep-ref deposition scheme are considered. (left): Gaussian cost function. (right): Log-normal cost function. Purple triangles represent the location of the Mayak and Dimitrovgrad sites. Blue dots are the 336 potential source locations.

Outside the southern Urals, there is a fairly wide geographical area in which FAC2 values are ranged from 30% to 40%, extending from the northern Urals to the western part of the Russian Federation. Furthermore,

the probability of the release occurred from Europe is very low. On the other hand, it can be seen that the use of a log-normal cost function tends to restrict the geographical area where FAC2 values are higher. In that case, this area is limited to the region around the Mayak nuclear complex. Besides, very similar results are obtained when the Météo-France meteorological fields are used. Finally, the influence of the deposition scheme on the location of the release is negligible, the most plausible source location remains the same for all deposition schemes used.

Source terms

The Mayak nuclear complex is the only plant identified in the most reliable release area, we therefore estimated the source term by inverse modelling from the location of this facility. Similar to the previous section, we constructed 8 source-receptor matrixes from the Mayak site which represent all combinations of the two sources of meteorological data and the 4 deposition schemes. In total, we performed 16 inverse calculations (8 based on a lognormal cost function and 8 based on a Gaussian cost function) to obtain 16 source terms. Table 2 and Table 3 show that the total quantities of ^{106}Ru estimated by inverse modelling ranged from 118 to 578 TBq.

Table 2: Features of the inverted source terms assessed using Météo-France meteorological data and 4 deposition schemes. Source location is Mayak nuclear complex.

Source term	Gau dep-ref	Log dep-ref	Gau dep1	Log dep1	Gau dep2	Log dep2	Gau dep3	Log dep3
Total release (TBq)	578	247	581	249	481	170	484	173
Period of the release	23 – 24 (65%) 26 – 27 (28%)	26 – 27 (99%)	23 – 24 (65%) 26 – 27 (28%)	26 – 27 (99%)	23 – 24 (70%) 26 – 27 (26%)	26 – 27 (99%)	23 – 24 (70%) 26 – 27 (26%)	26 – 27 (99%)

Table 3: Features of the inverted source terms assessed using ECMWF meteorological data and 4 deposition schemes. Source location is Mayak nuclear complex.

Source term	Gau dep-ref	Log dep-ref	Gau dep1	Log dep1	Gau dep2	Log dep2	Gau dep3	Log dep3
Total release (TBq)	541	164	547	167	367	115	373	118
Period of the release	23 – 24 (20%) 24 – 25 (64%)	24 – 25 (20%) 25 – 26 (68%)	23 – 24 (21%) 24 – 25 (63%)	24 – 25 (21%) 25 – 26 (67%)	23 – 24 (13%) 24 – 25 (73%)	24 – 25 (30%) 25 – 26 (60%)	23 – 24 (14%) 24 – 25 (71%)	24 – 25 (30%) 25 – 26 (59%)

It can be seen that the choice of meteorological fields has a moderate impact on the total estimated quantities. The results highlight that the source terms assessed using the ECMWF meteorological fields are slightly smaller than those estimated using the Météo-France meteorological fields, sometimes 30% smaller when a log-normal cost function is used. Moreover, the choice of the cost function has a significant impact on the source term estimated by inverse modelling. Indeed, we notice that the source terms assessed using Gaussian cost function are systematically higher, on average by a factor of 3, than the source terms obtained using a log-normal cost function. This phenomenon is explained by the priority given to high concentrations to the detriment of lower concentrations when a Gaussian cost function is used. This results in a good reproduction of the observations located in Italy ($>30 \text{ mBq/m}^3$) whereas the observed concentrations in Southern Europe (Greece, Turkey) and in Siberia ($< 5 \text{ mBq/m}^3$) are clearly overestimated. Finally, the impact of the deposition scheme is relatively small on the estimated atmospheric quantities. However, it seems that a deposition scheme associated with a dry deposition velocity of 0.1 cm.s^{-1} leads, as expected, to slightly lower source terms.

According to the simulations, the release period and its duration vary significantly depending on the meteorological fields and the cost function used. For the same meteorological data, there are significant differences depending on the choice of the cost function. For example, the duration of the release is 48 hours when Météo-France meteorological fields and a Gaussian cost function are used. This duration is

reduced to 24 hours when a log-normal cost function is taken into account. The use of ECMWF meteorological fields leads to the same phenomenon. The duration of the release is even extended to 72h and the maximum daily release occurs on September 24th using a Gaussian cost function whereas the maximum daily release is on September 25th using a log-normal cost function. Finally, the choice of the deposition scheme has a very small impact on either the period or the duration of the release.

Model-to-data comparison

The 16 source terms assessed by inverse modelling were used to simulate the ¹⁰⁶Ru plume dispersion from the Mayak site. Table 3 and Table 4 show that the FAC2 scores for air concentrations vary between 37% and 50% respectively, while the FAC5 scores are ranged from 65% to 73%. These scores demonstrate that the majority of the simulations are able to reproduce satisfactorily the observations. Furthermore, the meteorological fields have a strong influence on the scores. Indeed, the use of ECMWF meteorological fields gives higher scores than the Météo-France meteorological data. Similarly, it appears that the highest scores are obtained when the log-normal cost function is implemented together with ECMWF meteorological fields. Moreover, the influence of the deposition scheme remains limited even if dry deposition velocity of 0.1 cm.s⁻¹ allows to reach the highest FAC2 values, around 50%. The scores related to ¹⁰⁶Ru deposition measurements are relatively similar for all the simulations. The FAC2 values vary respectively between 21% and 33% while the FAC5 values range from 48% to 66%. These scores are lower than those obtained for air concentrations. Furthermore, the meteorological fields have no significant impact on the scores, which are of the same order of magnitude. Finally, it is difficult to identify one deposition scheme as being more relevant than another since the scores remain close to each other. We note, however, that the wet deposition scheme combining different in-cloud and below-cloud scavenging coefficients (dep1 and dep3 deposition schemes) slightly enhances the ability of the transport model to reproduce deposition measurements.

Table 4: Scores for ¹⁰⁶Ru air concentration and surface deposition results. Simulations are performed using Météo-France meteorological data. The best score is highlighted in green.

	Gau dep_ref	Log dep_ref	Gau dep1	Log dep1	Gau dep2	Log dep2	Gau dep3	Log dep3
FAC 2 (%) Air concentration	37	37	38	37	41	37	41	38
FAC 5 (%) Air concentration	67	65	67	65	68	66	70	66
FAC 2 (%) deposition	21	19	27	23	23	23	31	33
FAC 5 (%) deposition	63	63	58	63	60	63	56	59

Table 5: Scores for ¹⁰⁶Ru air concentration and surface deposition results. Simulations are performed using ECMWF meteorological data. The best score is highlighted in green.

	Gau dep_ref	Log dep_ref	Gau dep1	Log dep1	Gau dep2	Log dep2	Gau dep3	Log dep3
FAC 2 (%) Air concentration	47	47	46	48	50	50	49	50
FAC 5 (%) Air concentration	69	72	70	73	72	72	70	73
FAC 2 (%) deposition	21	23	21	29	27	25	27	27
FAC 5 (%) deposition	48	60	60	66	54	60	63	63

CONCLUSION

Variational inverse methods are relevant to reconstruct a source of unknown geographical origin. On the ¹⁰⁶Ru detection event, inverse methods combining several meteorological fields and deposition schemes allow to point out the southern Urals as the likely origin of the release with a high level of confidence. In addition, the use of ECMWF meteorological fields characterised by higher spatial resolution significantly

improves the agreement between simulated and observed air concentrations. The inverse modelling process seems to be more efficient with a log-normal cost function. Finally, the impact of the deposition scheme remains relatively small on this case study even if we notice that a wet deposition scheme combining different in-cloud and below-cloud scavenging coefficients slightly improves the reproduction of deposition measurements. Future work includes the enhancement of the deterministic inverse modelling approach by taking into account all together deposition and air concentration measurements in the minimization process.

REFERENCES

- Dumont Le Brazidec J., M. Bocquet, O. Saunier and Y. Roustan, 2020: MCMC methods applied to the reconstruction of the autumn 2017 Ruthenium-106 atmospheric contamination source, *Atmospheric Environment: X*, **6**, 2020, 100071, ISSN 2590-1621, <https://doi.org/10.1016/j.aeaoa.2020.100071>.
- Masson, O., et al., 2018: Potential source apportionment and meteorological conditions involved in airborne ¹³¹I detections in January/February 2017 in Europe. *Environ. Sci. Technol.*, **52**, 8488–8500
- Masson, O., et al., 2019: Airborne concentrations and chemical considerations of radioactive ruthenium from an undeclared major nuclear release in 2017. *Proc. Natl. Acad. Sci. U.S.A.*, **116**, 16750–16759
- Quélo, D., M. Krysta, M. Bocquet, O. Isnard, Y. Minier, and B. Sportisse, 2007: Validation of the Polyphemus platform on the ETEX, Chernobyl and Algeciras cases. *Atmospheric Environment*, **41**, 5300–5315, <https://doi.org/10.1016/j.atmosenv.2007.02.035>.
- Quélo, D., J. Baboussadiambou Mamadou, A. Quérel and T. Doursout, 2021: Wet deposition modelling capabilities investigated through a comprehensive study of dose rate peaks events due to atmospheric radon, 20th International Conference on Harmonisation within Atmospheric Dispersion Modelling for Regulatory Purposes. Tartu, Estonia
- Saunier, O., A. Mathieu, D. Didier, M. Tombette, D. Quélo, V. Winiarek, and M. Bocquet, 2013: An inverse modeling method to assess the source term of the Fukushima Nuclear Power Plant accident using gamma dose rate observations, *Atmos. Chem. Phys.*, **13**, 11403–11421, <https://doi.org/10.5194/acp-13-11403-2013>.
- Saunier, O., D. Didier, A. Mathieu, O. Masson, J. Dumont Le Brazidec, 2019: Atmospheric modeling and source reconstruction of radioactive ruthenium from an undeclared major release in 2017., *Proc. Natl. Acad. Sci. U.S.A.*, **116** (50), 24991-25000; DOI: 10.1073/pnas.1907823116
- Tombette, M., E. Quentric, D. Quélo, J.P. Benoit, A. Mathieu, I. Korsakissok and D. Didier , 2014: A software platform for assessing the consequences of an accidental release of radioactivity into the atmosphere. International Radiation Protection Association congress, Geneva
- Tichý, O., M. Hýža, N. Evangelidou, and V. Šmídl, 2021: Real-time measurement of radionuclide concentrations and its impact on inverse modeling of ¹⁰⁶Ru release in the fall of 2017, *Atmos. Meas. Tech.*, **14**, 803–818, <https://doi.org/10.5194/amt-14-803-2021>
- Western, L., S. Millington, A. Benfield-Dexter and C. Witham, 2020: Source estimation of an unexpected release of Ruthenium-106 in 2017 using an inverse modelling approach. *Journal of Environmental Radioactivity*. 220-221. 106304. 10.1016/j.jenvrad.2020.106304.